Dielectric totally internally reflecting concentrators

XP 002012726

Xiaohui Ning, Roland Winston and Joseph O'Gallagher

G02B 19/00

Dielectric totally internally reflecting concentrators (DTIRCs) which can achieve concentrations close to the thermodynamically allowed limits are introduced. General design methodologies are given explicitly. Geometrical and optical properties of DTIRCs are discussed.

P.D. 15/11/87
p. 300-305 = 6

I. Introduction

A. General

An optical concentrating system can be characterized by its angular field of view and its entrance and exit apertures. The geometric concentration defined as the area ratio of entrance to exit is limited by the angular field of view. In a 3-D geometry, the maximum concentration (thermodynamic limit) for an optical system with a conical angular field of view of (half-acceptance angle) $\pm\theta_a$ is given by

$$C_{max} = n_1^2/n_2^2 \sin^2\theta_a, \quad (1)$$

where n_1 and n_2 are the refractive indices of the media in which the entrance and exit apertures are immersed, respectively.[1] It is also known that the concentration of most simple conventional optical systems (e.g., lens, mirrors) are far below these limits. An *f*/stop Fresnel lens falls short of these limits by a factor of $4f^2$ *in vacuo*.[2]

In the last two decades, intensive research has been carried out in designing concentrators (in both 2-D and 3-D geometry) which have concentrations achieving or approaching these limits.[1,3] A well-known example of such a concentrator is the compound parabolic concentrator (CPC) which has been used in solar energy concentration systems[4] and high-energy Cherenkov light detectors.[5]

In this paper, we will discuss a new family of optical elements, dielectric totally internally reflecting concentrators (DTIRCs). DTIRCs combine the front surface refraction with total internal reflection from the sidewall to achieve concentrations close to the theoretical maximum limits. Compared with CPCs, because of the larger refractive index of dielectric and the use of a curved front surface, DTIRCs have two advantages: higher concentrations and smaller sizes. They can be used in many areas, e.g., solar energy concentrators and fiber optics, where the concentration or efficient transport of light is required. For example, the dielectric CPC (DCPC) has been developed as a single-element photovoltaic concentrator.[6,7]

In Sec. II, we will discuss the general design methodologies for DTIRCs. Their geometrical and optical properties will be analyzed in detail and comparisons to experimental data made in the following sections.

B. Nomenclature

θ_a = acceptance angle;
d_1 = entrance aperture;
d_0 = exit aperture;
φ = front surface arc angle;
n = index of refraction.

II. General Design Method of DTIRCs

When light rays are incident on a boundary of a medium of higher refractive index from one with a lower index at an angle greater than the so-called critical angle, the rays will all be reflected back to the region with a higher index. This physical phenomenon is known as total internal reflection (TIR), and the critical incident angle θ_c is derived from Snell's law:

$$\theta_c = \sin(n_1/n_2), \quad (2)$$

where n_1 and n_2 are refractive indices and $n_1 < n_2$.

It is possible to design a solid dielectric concentrator in which the condition for TIR is fulfilled at the side profile boundary for all rays incident on the concentrator within the design acceptance angle. Since it uses total internal reflection properties of the dielectric medium, it is known as DTIRC. A DTIRC consists of three parts: the front surface which may be curved; the totally internally reflecting sidewall (profile); and the exit aperture. Only rays within the design acceptance angle (corresponding to an angular field of view) need reach the exit aperture. Most rays incident on the front surface beyond the acceptance angle will eventually exit from the side profile. Rays incident at the acceptance angle are known as extreme rays, and they play an important role in determining the side profile of DTIRC. As for CPCs, we will solve the 2-D case and form 3-D DTIRCs by rotating the 2-D profile about its symmetry axis. In this paper, we will princi-

The authors are with University of Chicago, Enrico Fermi Institute, Chicago, Illinois 60637.

Received 9 July 1986.
0003-6935/87/020300-06$02.00/0.

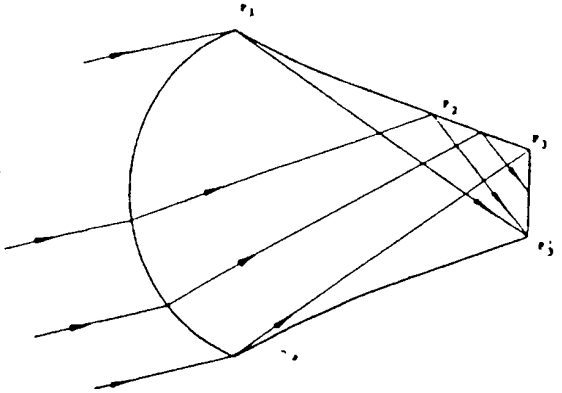

Fig. 1. Side view of a DTIRC. The extreme rays hitting the portion P_1P_2 converge into P'_3. Rays hitting the portion P_2P_3 can exit at whatever angle barely satisfies TIR (the maximum concentration method) or in parallel (the phase-conserving method).

pally be concerned with the properties of the 3-D solutions.

Figure 1 shows an example of a DTIRC. A set of rays incident on the front surface at the extreme angle is shown. Each passes through the front curved surface, is refracted, and subsequently is totally internally reflected from the sidewall and eventually hits the exit aperture. In determining the side profile, we maximize the slope of the side profile curve consistent with reflecting the extreme entrance rays after refraction by the curved front surface onto the exit subject to various subsidiary conditions we may wish to impose. For example, in addition to TIR, we may require rays to exit with an angle not exceeding a predetermined angle. DTIRCs generated in this subsidiary condition can be used in fiber optics where rays must enter fiber at angles smaller than a certain critical angle for transmission.

We will discuss two design methods for DTIRCs. In the first method, referred to as the maximum concentration method, there are no subsidiary conditions other than TIR imposed, and it yields the maximum achievable concentration with TIR. In the second method, the exiting extreme rays are parallel, that is, they form a new wavefront. This approach is referred to as the phase-conserving method.

Let us consider the example shown in Fig. 1. For simplicity (in both designing and manufacturing), we will restrict ourselves to the case where the front surface is a portion of a sphere. In general, we can divide the side profile into two parts: the portion from P_1 to P_2 and the portion from P_2 to P_3. Between P_1 and P_2, all extreme rays are directed to the corner P'_3 after a single TIR. The ray hitting P_2 just barely satisfies TIR and exits from P'_3. Between P_2 and P_3, the refractive index is not high enough to totally reflect the extreme rays to P'_3. There are two ways to design the profile in this region. One can simply require that TIR be maintained and allow the reflecting rays to assume whatever direction results as long as they strike the exit aperture. This results in a distribution of exit angles for the extreme incident angles and develops

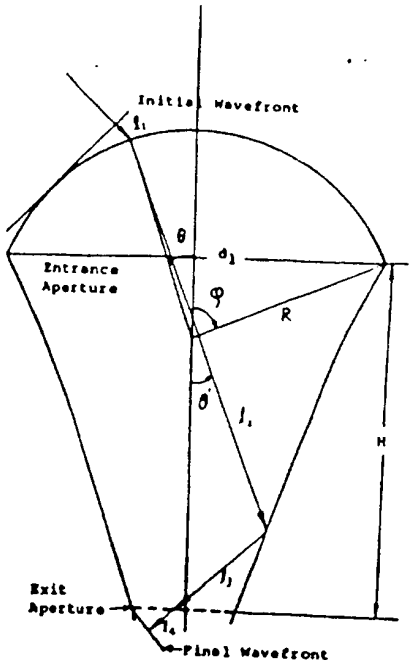

Fig. 2. Typical optical path consists of four parts: l_1, l_2, l_3, and l_4. For rays converging at the bottom left-hand corner, the portion l_4 is zero.

the maximum possible concentration achievable with an edge ray solution incorporating TIR. The second method is to slope the profile so that the reflecting rays are all parallel to one another with a direction corresponding to the line from P_2 to P'_3. This means that the extreme rays reflected from the portion between P_2 and P_3 emerge with a well-defined wavefront.

The two methods yield solutions which are very similar geometrically, but the advantage of the latter is that an analytical solution can be determined. That is, since extreme rays reflected from portion P_1P_2 of the profile converge onto a point and rays from the portion P_2P_3 exit in parallel. Fermat's principle can be used to generate the coordinates of the side profile. In general, the total optical path length of a ray from the entrance wavefront to the exit wavefront consists of four parts: l_1, l_2, l_3, and l_4 as shown in Fig. 2. The initial wavefront is shown just tangent to the curved front surface. The portion l_1 is from a point on the initial wavefront to the surface of DTIRC, l_2 is from there to the reflection point, l_3 is from the reflection point to the exit of DTIRC, and l_4 is from the exit of DTIRC to the final wavefront. For rays converging to P'_3, l_4 is zero.

According to Fermat's principle the total optical path length is a constant for every ray connecting the initial and final wavefront. Thus we have

$$\int n\,ds = l_1 + n(l_2 + l_3) + l_4 = \text{const.} \tag{3}$$

Combining Eq. (3) with DTIRC height and length constraints, we can solve for l_1, l_2, l_3, and l_4. Then the profile coordinates can be calculated analytically. The detailed relationships are derived in the Appendix. With the maximum concentration method, rays

from portion P_1P_2 are still convergent to P'_3. Thus the method outlined above is still applicable. But for portion P_2P_3, conserving the optical path can no longer be applied, since there is no well-defined wavefront. Recursion relations are developed to calculate the coordinates of the side profile. The detailed formulations are also shown in the Appendix.

We have developed computer programs to generate the side profile curves numerically. The programs require as inputs the front surface arc angle, the refractive index of the dielectric, the exit aperture, and the acceptance angle. The programs assume a trial entrance aperture and, therefore, trial height, then step through a set of extreme rays (where the total number of extreme rays depends on the precision requirement) to calculate coordinates of the DTIRC profile. It begins with the extreme ray reflected at P_3 and ends with the extreme ray entering the edge of the entrance aperture at P_1. The program then compares the entrance aperture generated with the trial aperture. The difference between two entrance apertures is used to adjust the trial aperture and height, and the procedure iterates until the trial aperture and calculated aperture converge to within a predetermined error tolerance. The entrance aperture is then defined, and X-Y coordinates of the DTIRC are calculated. The number of extreme rays determines the number of coordinates and also the numerical precisions. The following discussions are based on numerical solutions for DTIRCs which have 200 pairs of X-Y coordinates for the side profile.

When the radius of curvature of the spherical surface is small, we can treat the surface as an ideal lens which images the extreme pencil onto a point. In this approximation, for DTIRs designed using the maximum concentration method, the portion between P_1, P_2 is a hyperbola, while the portion between P_2P_3 is an arc of an equiangular spiral (see Fig. 3).

III. Geometrical Properties of DTIRCs

As indicated above there are four degrees of freedom in designing a DTIRC. Among these, the refractive index and the exit aperture are fixed in most situations. Thus we will focus our discussion on the effects caused by variations on the acceptance angle and front arc angle. It is found that the geometrical concentration defined as the area ratio of the entrance to exit depends not only on the acceptance angle but also the front arc angle, and this holds for DTIRCs designed using either method. In the phase-conserving method, we require not only that extreme rays satisfy TIR but also exit in parallel. Thus with the same front arc angle, DTIRCs generated using the phase-conserving method have a slightly lower concentration than DTIRCs using the maximum concentration method. Table I compares the concentrations for DTIRCs generated using the two methods at various acceptance angles.

The TIR condition is more difficult to satisfy as the front surface becomes more curved because rays are bent more sharply. Thus the concentration becomes

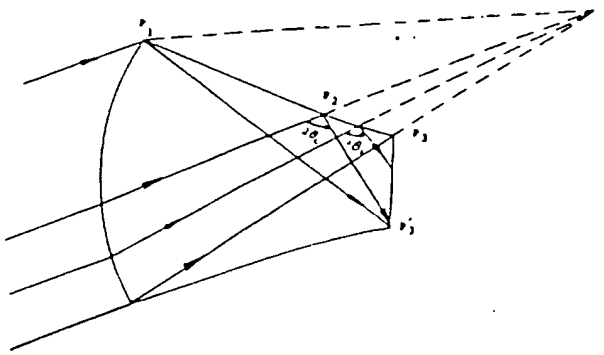

Fig. 3. When the front surface curvature is small, the portion P_1P_2 is just a hyperbola, and the portion P_2P_3 is just an arc of an equiangular spiral.

Table I. Comparison of Concentrations (Index = 1.5, Arc Angle = 30°, Exit Aperture = 1 cm)

Acceptance angle (deg)	Phase-conserving method	Maximum concentration method
18.0	21.81	22.09
20.0	17.56	17.81
22.0	14.44	14.67
24.0	12.11	12.32
26.0	10.24	10.43
28.0	8.76	9.00

Table II. Concentrations vs Arc Angle (Index = 1.5, Acceptance Angle = 22°, Exit = 1 cm)

Arc angle (deg)	Phase-conserving method	Maximum concentration method
10	15.37	15.44
20	14.98	15.05
30	14.44	14.67
40	13.84	14.36
45	13.47	14.29
50	13.10	14.21

smaller for a DTIRC as the front arc angle is increased. Table II shows the concentrations for DTIRCs with different front surface curvatures for a fixed acceptance angle for both maximum concentration and phase-conserving methods. From Tables I and II, it is obvious that DTIRCs generated using the maximum concentration method have slightly higher concentrations. DTIRCs designed using this method are preferred in applications where concentration is the only concern, i.e., solar energy photovoltaic concentrators.[2,8] Since for DTIRCs designed using the phase-conserving method, the maximum exiting angle is expressed in terms of the four input parameters analytically, we can choose appropriate parameters in designing DTIRCs so that no ray will exit with an angle larger than a predetermined angle. DTIRCs with a maximum predetermined exiting angle can be used in fiber optics where the angular requirement is crucial.

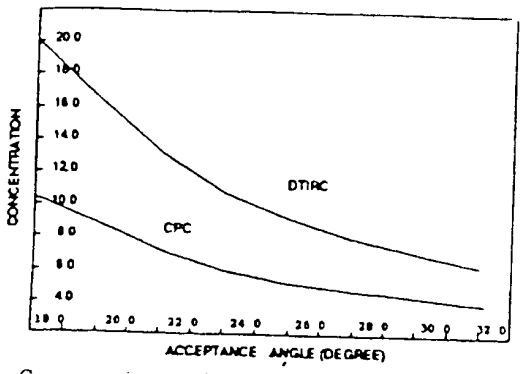

Fig. 4. Concentrations as functions of one acceptance angle for both DTIRC and CPC. With the same acceptance angle, DTIRC has a higher concentration.

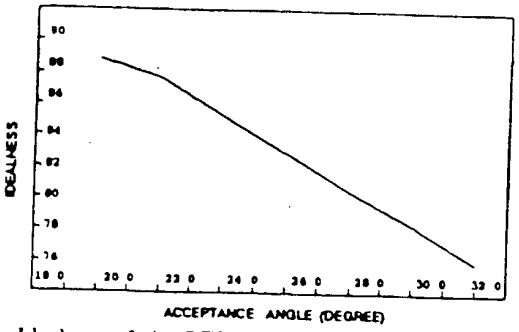

Fig. 5. Idealness of the DTIRC decreases with the acceptance angle, while the idealness of CPC is one.

Despite all these comments, the geometrical differences between DTIRCs designed using different methods are quite small. Especially for the DTIRCs with a smaller acceptance angle and/or smaller front curvatures, the difference is insignificant in practical applications. In the following discussions, we will only consider DTRICs designed using a maximum concentration method.

Figure 4 shows the geometrical concentrations of a mirror-constructed CPC and DTIRCs designed for various angular acceptances. If one defines idealness as the ratio of geometrical concentration of a DTIRC to the maximum limit given by Eq. (1) for a given acceptance angle, a quantitative relationship between idealness and the acceptance angle for a DTIRC is shown in Fig. 5. Since total internal reflection is not required for CPC, its idealness is one. We can see from Fig. 5 that the smaller the acceptance angle is, the closer the DTIRC is to the thermodynamic limit. Unlike CPCs, the curved front surface of DTIRC functions like a lens which concentrates before the rays are reflected. Apparently, the more curved the front surface, the shorter the DTIRC. Figure 6 shows a family of DTIRCs with different front surface curvatures for a given acceptance angle. A dielectric CPC (DTIRC with a flat front entrance) is also shown. The front surface curved DTIRCs are much smaller. If one defines the DTIRC height as the distance from the exit to the top of the side profile and total height from the exit to the top of the curved front surface, quantitative

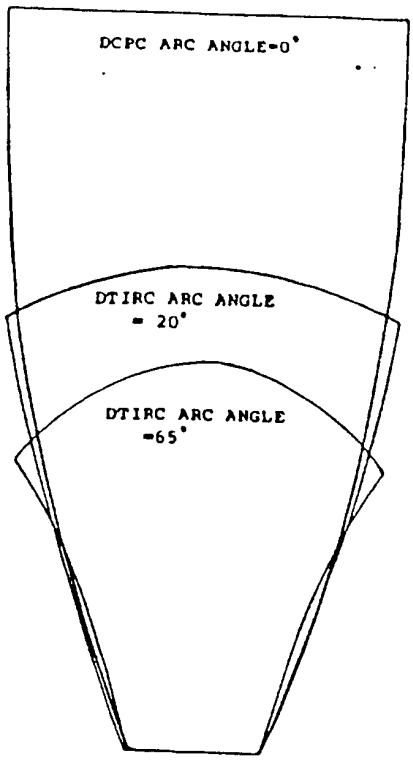

Fig. 6. Family of DTIRCs with a different front surface arc angle. Because of curved front surfaces, DTIRCs can be made smaller.

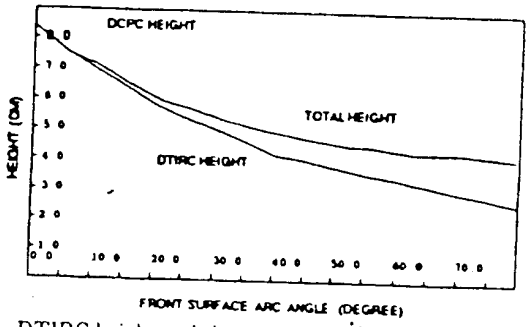

Fig. 7. DTIRC height and the total height decrease with the front surface arc angle.

relations between heights of DTIRCs and front arc angles are shown in Fig. 7.

We should point out that as the front surface varies from a small curvature to a larger one, the side profile of DTIRC changes from convex to concave. This suggests the possibility that with a certain front curvature the side profile of DTIRC can be well approximated by a straight line. In fact this turns out to be the case. Straight side DTIRCs are expected to be easier to produce. Table III shows the linear correlation coefficient r of the side profile of DTIRC at various front curvatures.[9] As one can see from this table, the side profile of DTIRC can be very well approximated by a straight line for a front surface arc angle of ~50°. If we relax the requirement that the front surface be spherical, it is possible that the side profile is exactly a straight line in certain circumstances. Aspherical front curved DTIRC will be discussed in a later paper.

Table III. Arc Angle vs Linear Correlation Coefficient (Index of Refraction = 1.47, Acceptance Angle = 22°)

Arc angle (deg)	Coefficient r
10	0.95910
20	0.98268
30	0.99326
40	0.99814
45	0.99925
50	0.99966
55	0.99945
60	0.99862
65	0.99723

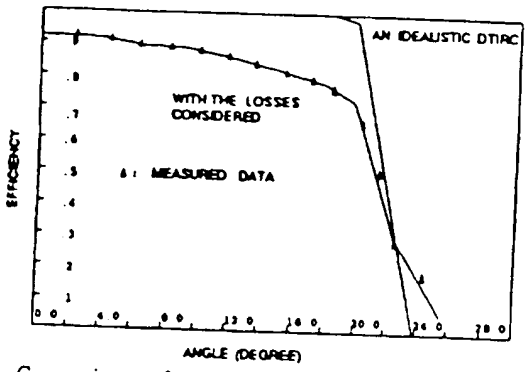

Fig. 8. Comparisons of computer simulated angular acceptance curves with data for a DTIRC with a design acceptance angle of 21.64°.

IV. Optical Properties of DTIRC

The optical performance of DTIRC can be best described by its angular acceptance. The angular acceptance curve is defined as the normalized optical throughput vs light incident angle θ. The angular acceptance curve for DTIRC is very similar to CPCs and has a clear cutoff at the designed acceptance angle. Figure 8 shows a computer simulated angular acceptance curve for a physically ideal DTIRC designed for an acceptance angle equal to 21.64°. The rounding and sloping falloff of the ideal DTIRC in the angular acceptance curve is due to skew ray losses. The angular acceptance can also be determined experimentally. We measured a DTIRC designed with an acceptance angle of 21.64°, front arc angle of 65°, and an exit aperture of 1 cm. A 1-cm diam solar cell optically coupled to the exit of the DTIRC was used as the optical throughput detector. The experiment was done in sunlight on a clear day. Because the cell short circuit current is proportional to the amount of light it receives, by measuring the cell short circuit current at different angles, the angular acceptance can be determined after the effects of diffuse sunlight are corrected. The normalized throughput F as a function of incident angle θ can be expressed as

$$F(\theta) = I_b(\theta)/I_c/C_g, \tag{4}$$

where I_b is the short circuit current with DTIRC normalized to beam insolation, I_c is the cell alone short circuit current normalized to total insolation, and C_g is the geometrical concentration of the DTIRC, which is 13.6 in this case.

A computer model was also developed which calculates the effects of front surface reflection, absorption in the dielectric, and the reflections at the dielectric–cell interface. Figure 8 also shows the comparisons of computer simulations with the measured data. From this figure, it is clear that theory and experiment agree well.

V. Conclusions

A new class of dielectric total internal reflection concentrator designed according to optical principles has concentrations approaching the theoretical maximum limits. Compared with CPCs, DTIRCs offer higher concentrations and smaller physical sizes, which are important in practical applications. Since subsidiary conditions can be imposed on designing DTIRCs, they can be designed to meet various kinds of requirements in situations where concentrations are necessary. Applications of DTIRCs as a secondary concentrator in photovoltaic systems will be discussed in the future.

This work is supported in part by the U.S. Department of Energy and the SOLERAS program under grant DE-FGO2-84CH 10201. We wish to thank Peter Gruenbaum for developing part of the mathematical formulations.

Appendix: Mathematical Formulations

A: Phase-Conserving Method

Given a wavefront of extreme rays, the part of it which hits portion P_1,P_2 of the side profile of DTIRC is reflected into the bottom corner P_3. Another part which hits portion P_2,P_3 must leave the aperture as a new wavefront. If we use l_i (i = 1,2,3,4) for different parts of the optical path shown in Fig. 2, then, according to Fermat's principle, the optical path length $C = l_1 + n(l_2 + l_3 + l_4)$ must be a constant.

The radius of front curvature R can be expressed in terms of front arc angle φ and entrance diameter d_1 by the following equation:

$$R = d_1/(2\sin\varphi). \tag{A1}$$

Now consider an extreme ray which hits the front surface corresponding to an arc angle θ shown in Fig. 2. This ray will leave the front surface with an angle θ' relative to vertical axis:

$$\theta' = \sin^{-1}[\sin(\theta + \theta_a)/n] - \theta. \tag{A2}$$

And the optical path l_1 is given by

$$l_1 = 2R\sin[(\theta + \theta_a)/2]. \tag{A3}$$

Using the fact that the ray from P_1 should hit P_3, DTIRC height H can be determined. Using Eq. (A2), it can be shown that

$$H = \tfrac{1}{2}(d_1 + d_2)\cot(\Theta), \tag{A4}$$

where $\Theta = \max(\theta') = \sin^{-1}[\sin(\theta_a - \varphi)/n] + \varphi$, and the optical path C is given by

$$C = 2R\sin^2[(\theta_a + \varphi)/2] + n(d_1 + d_0)/[2\sin(\Theta)]. \quad \text{(A5)}$$

If θ is such that the ray hits portion P_1,P_2 of the side profile, the ray goes into P'_3 and $l_4 = 0$. We have three unknowns (l_2,l_{3x},l_{3y}) and three equations:

$$\text{Optical path length:}\quad C = l_1 + n[l_2 + (l_{3x}^2 + l_{3y}^2)^{1/2}]; \quad \text{(A6)}$$

$$\text{Height:}\quad l_2\cos(\theta') + l_{3y} - R[\cos(\theta) - \cos(\varphi)] = H; \quad \text{(A7)}$$

$$\text{Length:}\quad R\sin(\theta) + l_2\sin(\theta') - l_{3x} = -d_0/2. \quad \text{(A8)}$$

From these equations l_2 can be solved:

$$l_2 = \{[(c - l_1)/n]^2 - [R\sin(\theta) + d_0/2]^2 - H^2\}/$$
$$\{(c - l_1)/n + [R\sin(\theta) + d_0/2]\sin\theta' - H\cos\theta'\}. \quad \text{(A9)}$$

The extreme rays hitting a portion of the P_2,P_3 exit with the same angle θ_0, which is determined by requiring that the ray from P_1 to P'_3, just barely satisfies the TIR condition at P_2. And the exit angle θ_0 is given by the following formula:

$$\theta_0 = \pi - \Theta - 2\theta_c, \quad \text{(A10)}$$

Where θc is a TIR critical angle given by Eq. (2).

Once again we have three unknowns (l_2,l_3,l_4) and three equations:

$$\text{Optical path length:}\quad C = l_1 + n(l_2 + l_3 + l_4); \quad \text{(A11)}$$

$$\text{Height:}\quad l_2\cos(\theta') + l_3\cos(\theta_0) = H; \quad \text{(A12)}$$

$$\text{Length:}\quad R\sin(\theta) + l_2\sin(\theta') - l_3\sin(\theta_0) = -d_0/2 + l_4/\sin(\theta_0). \quad \text{(A13)}$$

To solve these equations, we obtain

$$l_2 = \{(C - l_1)/2 - H/\cos(\theta_0) - [R\sin(\theta) - H/\cos(\theta_0) + d_0/2]\sin(\theta_0)\}/$$
$$[1 - \cos(\theta')/\cos(\theta_0) + \sin(\theta')\sin(\theta_0) + \cos(\theta')\sin(\theta_0)\tan(\theta_0)], \quad \text{(A14)}$$

$$l_3 = [H - l_2\cos(\theta')]/\cos(\theta_0), \quad \text{(A15)}$$

$$l_4 = [R\sin(\theta) + l_2\sin(\theta') - l_3\sin(\theta_0) + d_0/2]\sin(\theta_0). \quad \text{(A16)}$$

Once we have l_2, then x and y coordinates are given as follows:

$$x = R\sin(\theta) + l_2\sin(\theta'); \quad \text{(A17)}$$

$$y = H - l_2\cos(\theta') + R[\cos(\theta) - \cos(\varphi)]. \quad \text{(A18)}$$

B: Maximum Concentration Method

Compared with the phase-conserving method, the maximum concentration method does not require rays hitting a portion P_2,P_3 of the side profile exiting with the same angle. For rays hitting a portion P_1,P_2, the methodology is the same for both phase-conserving and maximum concentration. Thus the formula derived above for the portion P_1,P_2 [Eqs. (A1)–(A9)] is still applicable. We will focus on discussions on the portion P_2,P_3 where there is no longer a clearly defined wavefront.

Assume that a point with coordinates (X_i,Y_i) in the portion P_2,P_3 has been determined. The next point (X_{i+1},Y_{i+1}) is just the intersection of the next extreme ray with a straight line extending from (X_i,Y_i) with such a slope that this ray will just be totally internally reflected. It can be shown that (X_{i+1},Y_{i+1}) is connected to (X_i,Y_i) by the following recursion relations:

$$X_{i+1} = [H + R\sin(\theta) - Y_i + X_i\tan(\theta_c + \theta') - R\sin(\theta)\cot(\theta')]/$$
$$[\tan(\theta_c + \theta') - \cot(\theta')]; \quad \text{(B1)}$$

$$Y_{i+1} = (X_{i+1} - X_i)\tan(\theta_c + \theta') + Y_i. \quad \text{(B2)}$$

Let us use N as the number of total extreme rays which determines the solution precisions. In the computer program, one starts with P_3, which has coordinates $(0,d_0/2)$. The next point is determined by considering the next extreme ray, which hits the front surface corresponding to an arc angle $\theta = -(N-1)/N\varphi$. Then the next extreme ray is traced in the same fashion until a ray exits P'_3. Then the phase-conserving formulations are used.

References

1. W. T. Welford and R. Winston, *The Optics of Nonimaging Concentrators, Light and Solar Energy* (Academic, New York, 1978), p. 24.
2. J. O'Gallagher and R. Winston, "Nonimaging Dielectric Elements in Second Stage Concentrators for Photovoltaic System," in *Proceedings, Annual Meeting ASES*, Minneapolis (1983), p. 941.
3. The literature is intensive: see, for example, J. C. Minano, J. M. Ruiz, and A. Luque, "Design of Optimal and Ideal 2-D Concentrators with the Collector Immersed in a Dielectric Tube," Appl Opt. 22, 3960 (1983); R. Winston and W. T. Welford, "Geometrical Vector Flux and Some New Nonimaging Concentrators," J. Opt. Soc. Am. 69, 532 (1979).
4. R. Winston, "Principles of Solar Concentrators of a Novel Design," Sol. Energy 16, 89 (1974).
5. H. Hinterberger and R. Winston, "Efficient Light Coupler for Threshold Cerenkov Counter," Rev. Sci. Instrum. 37, 1094 (1966).
6. R. Winston, "Dielectric Compound Parabolic Concentrators," Appl. Opt. 15, 291 (1976).
7. R. L. Cole, A. J. Gorski, R. M. Graven, W. R. McIntire, W. W. Schertz, R. Winston, and S. Zwerdling, "Application of Compound Parabolic Concentrators to Solar Photovoltaic Conversion," Argonne National Laboratory Report ANL-77-42 (1977).
8. R. Winston, X. Ning, and J. O'Gallagher, "Photovoltaic Concentrator with Dielectric Second Stage," in *Proceedings, Annual Meeting ASES*, Boulder CO (1986), p. 417.
9. The linear correlation coefficient r is defined as $r = |N\Sigma X_iY_i - \Sigma X_i\Sigma Y_i|/|N\Sigma X_i^2 - (\Sigma X_i)^2]^{1/2}[N\Sigma Y_i^2 - (\Sigma Y_i)^2]^{1/2}|$ where N is the number of the (X,Y) pair. The value of r is ranged from 0, where there is no correlation to ±1, when there is complete correlation [see P. R. Bevington, *Data Reduction and Error Analysis for the Physica Sciences* (McGraw-Hill, New York, 1969), p. 121].